Development of the sensor and actuator node device for an autonomous ATV

Development of the sensor and actuator node device for an autonomous ATV

Mem. Muroran Inst. Tech., 62(2012) 59~65

特　　集

Development of the sensor and actuator node device for an autonomous ATV

Makoto KOBAYASHI*, Yuuta TOCHIKUBO*, Jun DAI*, and Naohiko HANAJIMA**

(Received 9 April 2012, Accepted 17 January 2013)

This paper addresses the development of sensor and actuator node device for an autonomous All Terrain Vehicle (ATV). Generally, the present field survey activities are performed by manual labors. The range of the field survey tends to be vast; therefore a lot of labors are needed. To realize the investigation of the environment with less manned labors, we add the functionality for automation to the ATV. In this paper, we introduce the CAN bus network to the autonomous ATV for the distributed control system, and construct the steering angle control system of the ATV and evaluated it.

Keywords : Environmental investigation，All Terrain Vehicle，Steering device，CAN

1 INTRODUCTION

There is an increasing demand on developing autonomous mobile robots for fieldwork such as a mine detection robot [1] , a robot which performs the cleanup activity of a nuclear power plant [2], an under-water robot [3], a planetary exploration robot [4], a rescue robot [5] and so on.

For field survey activities it is required to save working hours, work force and workers' health. We have chosen a commercially available All Terrain Vehicle (ATV) as the base of the autonomous vehicle and developed several devices for throttle control, brake control [6], speed measurement, and a wire-winding steering system [7]. In the study of autonomous vehicles using ATV, there is a UV (Unmanned Vehicle) project [8]. This project adopts drive-by-wire and steer-by-wire system. The steering system requires heavy customization. The wire-winding system can be easily attached or detached. When loosening the wire, drivers can interrupt the autonomous driving.

In present automobile, many micro computers are employed and CAN bus networks are widely introduced. In the field of robotics, the CAN bus networks are utilized recently. In the study of RT-Middleware [9], a CAN bus is introduced. However, implementing RT component on our ATV is not easy. Therefore we constructed a handmade CAN bus using microcontroller interfaces. The ATV has an automotive network using a CAN bus. Each device is connected to the CAN bus which has become possible to communicate with each of the data required for control. In addition, a constant-speed driving has been achieved in the speed control system.

In this paper, we introduce the CAN bus network to the autonomous ATV for the distributed control system,

Fig.1 ATV developed autonomous

* Division of Mechanical Systems and Materials Engineering, Muroran Institute of Technology
** College of Design and Manufacturing Technology, Muroran Institute of Technology

and construct the steering angle control system of the ATV and evaluated it.

2 CONFIGULATION OF THE ATV

2.1 Devices on the ATV

Figure 1 shows the ATV under developing in our laboratory. The base ATV (Suzuki Vinson LT-A500) has 493 cc SOHC engine, V-belt CVT automatic transmission with high/low range, and 2WD or 4WD modes. The body has two careers at the front and rear. Devices for autonomous running are installed on the front carrier.

A generator on the rear supplies AC 100 Volts for the devices on the front carrier. The steering device, motor driver, D-GPS, LIDAR sensor, gyro orientation sensor, terminal PC, microcomputer board, and so on are installed in the aluminum frame and the device protective cover on the front carrier. Rotary encoders mounted to rear wheel axis and the steering axis enable to measure the vehicle speed and the steering angle, respectively. Speed control device and brake control device on the left and right handle bar are attaced. The space on the rear carrier is reserved for the future development of environmental measurement equipments.

2.2 Steering system

Figure 2 shows the wire-winding steering system. In a wire-winding device, a DC-motor rotates the wire-winding shaft as shown in Figure 2(a). Two winding devices are attached to a both side of the aluminium frame as shown Figure 2(b). The winding devices and the handlebar ends are connected by wires. Winding one side of the wire gives a steering torque to the handle. Therefore, when steering, one motor winds one wire and the other loosens the other wire.

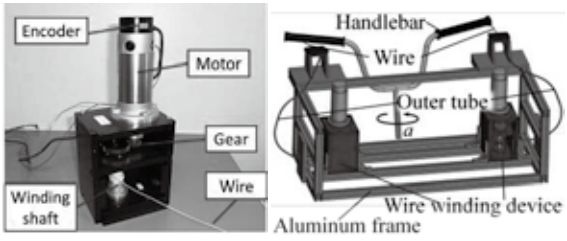

(a) Wire-winding device (b) Steering system

Fig.2 Wire-winding steering system

2.3 Control network

Figure 3 shows an automotive network before the introduction of CAN bus. In this network, all the control information is concentrated in the PC. In case of adding a new device, the PC needs to be provided a specific interface for the device and it increases the load of the PC. Therefore, a CAN bus is introduced in order to distribute the processing load.

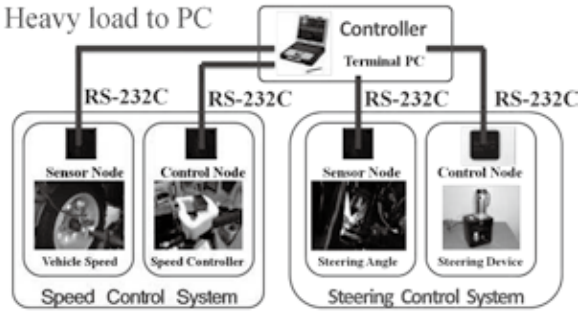

Fig.3 Former control network

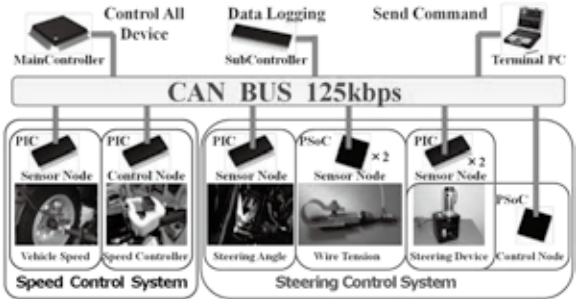

Fig.4 Current CAN bus control network

The features of CAN bus is high reliability, such as the determination of the multiple error detection elements, the judgment at the time of the error, and processing. Moreover, high-speed communication of up to 1 [Mbps] is available. It adopts a bus network topology so that wire-saving is possible compared to Figure 3.

Figure 4 shows the current automotive CAN bus network (ISO 11898 standard, baud rate: 125[kbps]) on the developing autonomous ATV. The sensor and control nodes are interface devices for the CAN bus, and consist of Cypress's PSoC CY8C3866-068, Microchip's PIC18F2580, PIC18F4580 and dsPIC30F6012A. The main controller (dePIC30F6012A) takes a role of calculation of the feedback control law. In the sensor nodes, PICs count the pulses from encoders and PSoCs manage A/D conversion. In the control nodes, a PIC manages the servo motor control (PWM output) of the throttle, and a PSoC the control of steering device. The main controller receives all sensor data, calculates and sends control commands to control nodes. Sub-controller performs the collection of data from the CAN bus and records the result on terminals, such as a PC. The PC transmits the control commands to the main controller.

From the next section, we describe the introduction of the CAN bus in the steering angle control system.

3 CONFIGURATION OF CONTRL DEVICE

3.1 PSoC

The PSoC (Programmable System-on-Chip) is a

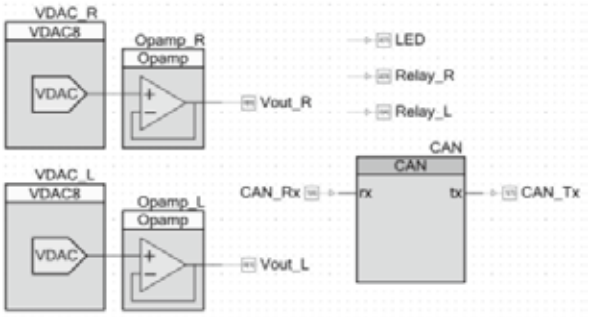

Fig.5 An example of PSoC's component design

microcontroller developed by Cypress Semiconductor. The integrated circuit of PSoC is composed of a core processor and configurable analog and digital blocks. Figure 5 shows a part of the program screen of PSoC. DA converter, Op-Amp, and CAN interface are shown. Integration of various analog and digital blocks realizes the sets of requred features.

In the steering control system shown in Figure 4, the PSoC devices (PSoC3 TEST BOARDs (IT Shop Etcetra, with CY8C3866-068)) are used to control the wire-winding steering system and to measure the wire tensions.

3.2 Steering device control node

Figure 6 shows the steering devices control node and motor drivers on a board. These are mounted in the aluminum frame of the ATV. The steering device control node was developed using the PSoC. It receives the control commands from the main controller through the CAN bus, and outputs directive voltages to the motor drivers (Sawamura Denki, SS40E6-E-L2-10 (24V)) in order to control the right and left wire-winding devices.

Figure 7 shows the flow of the control. The main controller sends control commands to the control node. According to the control commands, the PSoC outputs the directive voltages to the motor drivers. Then, the motor drivers operate the wire-winding devices.

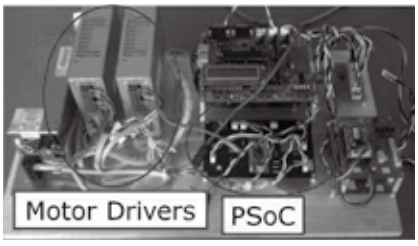

Fig.6 Electrical device for the steering control

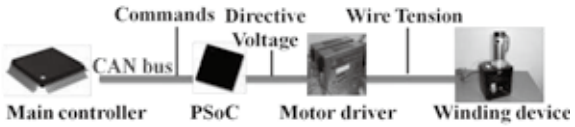

Fig.7 Structure and data flow of steering control

3.2.1 D/A converion and CAN communication

The PSoC device receives control commands in 8-bit digital data from the main controller through the CAN bus, and converts it to analog directive voltages to each motor driver. The directive voltage range to the motor driver is DC±10V. However, the PSoC voltage range is from 0[V] to +4.096[V]. Therefore, a level conversion circuit is developed and installed. Figure 8 shows the relationship between directive voltage and control command. We can estimate the directive voltage using the relationship.

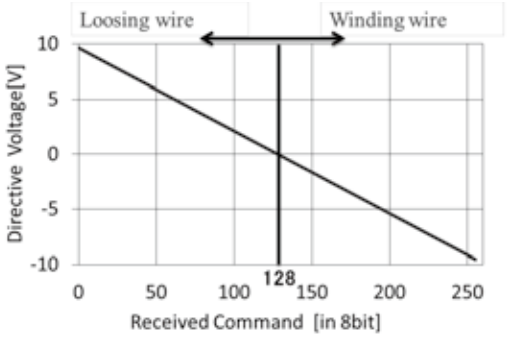

Fig.8 Relation between received command (digital) and directive voltage (analog)

3.2.2 Setting of the motor driver

Two motor drivers are mounted in order to operate the winding device of the left and right respectively. We have set the control mode of the both motor drivers to the current control, and tune the current limit trimmers so that each maximum wire tension is 200[N].

Figure 9 and Figure 10 show the relationship between the directive voltage and the actual wire

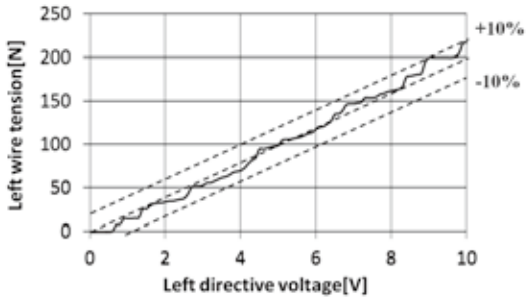

Fig.9 Left wire tension due to motor directive voltage

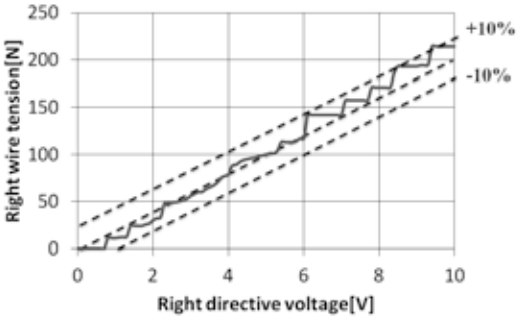

Fig.10 Right wire tension due to motor directive voltage

tension. There are the deflections of ±10% in each wire tension.

3.3 Wire tension measurement node

A wire tension measurement node obtains A/D converted value of the wire tension measured by the PSoC.

Figure 11 shows the wire tension sensor installed at the end of each wire. The sensor consists of a load cell (Measurement Specialties, ELFE-T4M-250N/Z1/AMP), a handlebar attachment and a wire connector. The handle attachment is fixed by tightening the bolt. The sensor is fixed in each handlebar, and the wire is connected so that the wire tension is applied to the load cell. The electrical signal from the load cell is connected to the sensor node. Its voltage of 0 [V] ~ 5 [V] corresponds output according to the tension of 0[N] ~200[N].

Figure 12 shows the flow of the measurement. The PSoC measures the wire tension by 14-bit A/D conversion of the voltage. The measured tension is transmitted to the main controller through the CAN bus. In this way, the main controller can get the wire tensions required to control the steering angle.

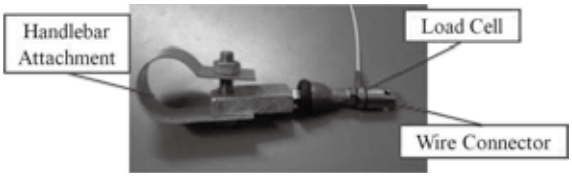

Fig.11 Composition of the tension sensor

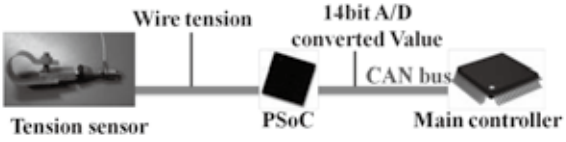

Fig.12 Structure and data flow of tension measurement

3.4 Waterproofing and dustproof case

The various devices on the ATV need to be protected for use in the outdoor environment.The steering device control nodes have been already mounted in the device protective cover on the front carrier.

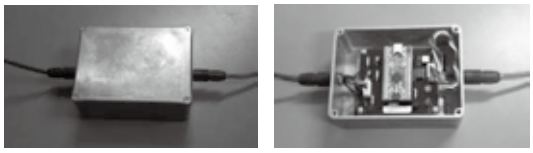

Fig.13 Wire tension measurement node in the sealed box

However, the tension measurement nodes are installed out of the front device protective cover. Then, we decided to store the node in a sealed aluminum box as shown in Figure 13. Moreover, the waterproof connectors are attached for wiring. The cable for wiring is composed of a 5 [V] power supply line, a ground line, and a CAN bus line.

4 FUNCTIONAL EVALUATION

4.1 Control system

Figure 14 shows the block diagram of the steering angle control. It is used for the portion of the wire tension control constituted from the foregoing paragraph. α is the steering angle, τ_m is the steering torque, T is the wire tension, $*$ indicates the target value, R and L indicate right and left device associated with the steering device respectively. The inner loop is composed of the wire tension controller C_{TR} and C_{TL}. The outer loop is composed of steering angle controller C_α. The PID controllers are used for these controllers. A target steering torque τ_m^* is calculated in C_α and converted into the wire tensions of the steering devices. To increase the holding force of the handle, the the offset tensions (preliminary tensions) T_R', T_L' are added to the wire tensions and we obtain the target value T_R^*, T_L^*. Then the deviation of T_R and T_R^*, T_L and T_L^* are input to C_{TR}, and C_{TL} respectively, and the motor torques τ_R, τ_L are output.

4.2 Test bed

We evaluated the feature of the steering angle control system before installing a real machine. Figure 15 shows the test bed [10], and Figure 16 does its schematic view. The winding devices and the handlebar are fixed

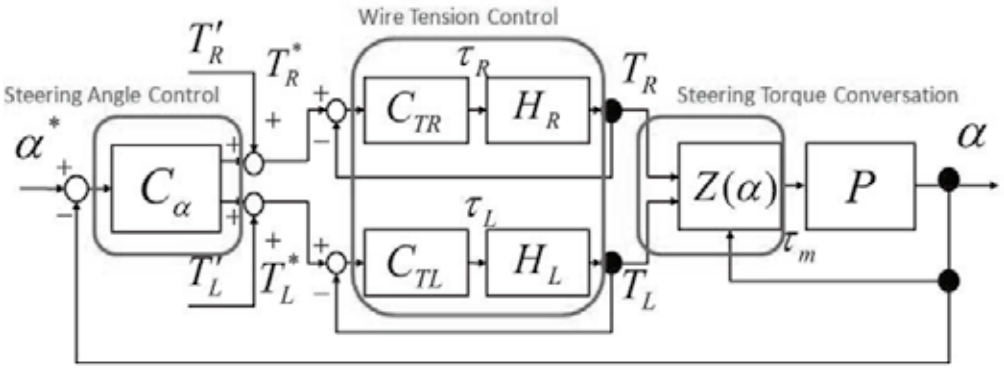

Fig.14 Block diagram of steering control system

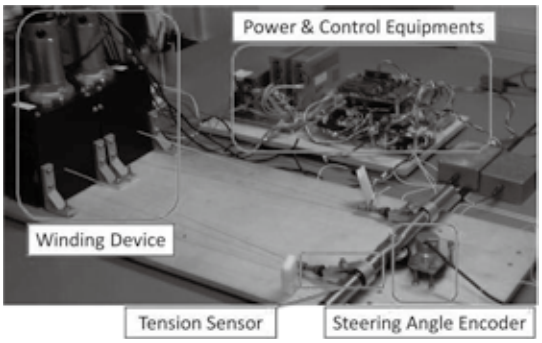

Fig.15 Test bed for steering control experiment

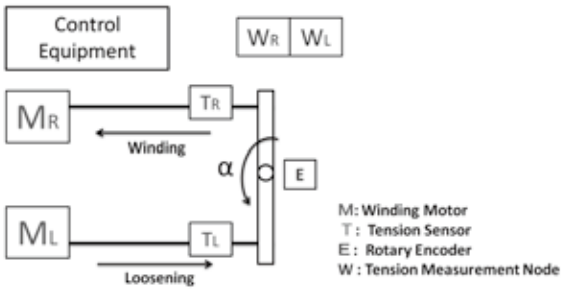

Fig.16 Schematic view of the test bed

on the wooden board. The handlebar is rotated by the wire-winding device. The rotation angle of the handle is measured by the encoder.

4.3 Estimating the transfer function

We estimated the transfer function of the wire-winding device by using the step response method.

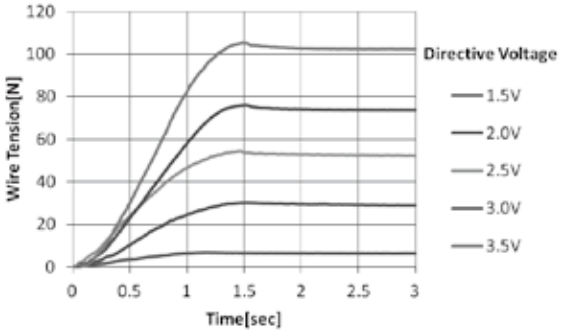

Fig.17 Step responses of the right steering device

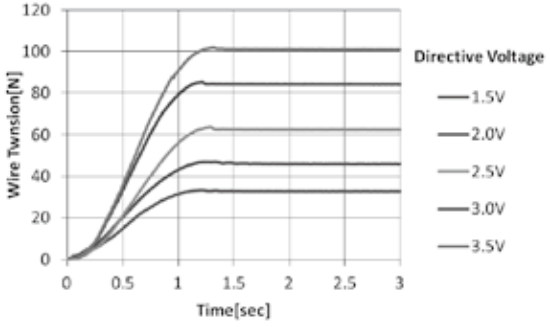

Fig.18 Step responses of the left steering device

We loosen the wire to set the wire tension 0 [N], and measure the change of the wire tension when the step input of directive voltage is given to the motor driver. The directive voltage to the motor driver is increased from 0 [V] to 3.5[V] by 0.5[V] step.

The following equation (1) shows the transfer function approximated by the second-order system, where ω_n is eigen frequency, ζ is damping coefficient.

$$H(s) = \frac{Y(s)}{X(s)} = \frac{{\omega_n}^2}{s^2 + 2\zeta\omega_n s + {\omega_n}^2} \quad (1)$$

Figure 17 and Figure 18 shows the step responses by the experiment of the steering device. The parameters ω_n and ζ can be identified from the step response method as shown in Table 1.

Table 1 Estimated parameters of the second-order system

	ω_n	ζ
Right winding motor	2.49	0.69
Left winding motor	2.61	0.71

The relationship of the motor torque of the steering device and the output wire tension is represented by the equation (2) and (3), where $H_R(s)$ is an estimated transfer function of the right device, $H_L(s)$ the left device.

$$H_R(s) = \frac{6.200}{s^2 + 3.436s + 6.200} \quad (2)$$

$$H_L(s) = \frac{6.812}{s^2 + 3.706s + 6.812} \quad (3)$$

4.4 Wire tension control experiment

We conducted the experiment to add the preliminary tension to the left and the right wires. The corresponding parts in Figure 14 are closed loops of C_{TR} and C_{TL}. At first the steering device is controlled at the constant wire winding speed 50 [mm/s]. After

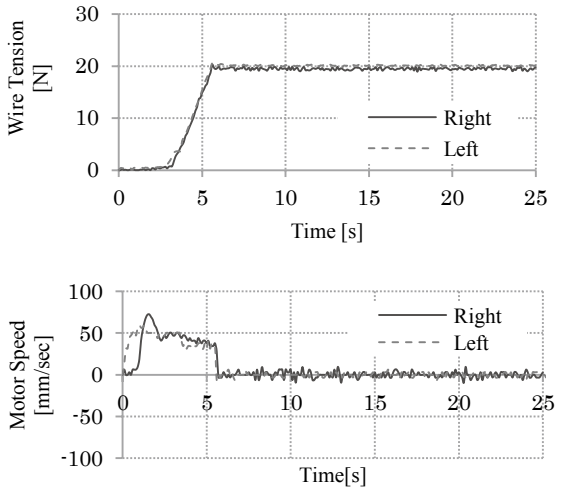

Fig.19 Wire tension control result of test bed experiment

reaching the target preliminary wire tension 20 [N] by winding the wire, it switches to the tension control.

The experimental results are shown in Figure 19. The graph shows the change of the wire tension and the winding speed. At first, the both motor speeds are kept around 50[mm/s], and the both wire tensions raise up to 20[N]. After 6 seconds, they are kept to the preliminary tension of 20[N]. From this experiment, we confirmed that it is possible to control the wire tension using the developed control system on the test bed.

4.5 Steering angle control experiment

We conducted the steering angle control experiment. The target steering angle 10 [deg] in the step input is given after adding a preliminary tension 20 [N] to the left and the right wires. The experimental results are shown in Figure 20. These graphs show the change of the wire tension and the steering angle. The graphs show the steering angle converges to the target angle. These experimental results show that the developed steering control system properly works on the test bed.

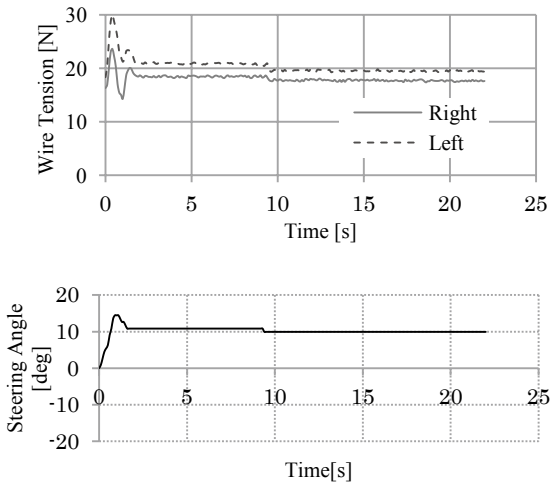

Fig.20 Steering angle control result of test bed experiment

5 DRIVING TEST

We installed the developed system and devices on the ATV and conducted the steering control experiment at the constant speed running.

The experiment was conducted in two kinds of fields, grass field and gravel field. The grass field is a certain flat place without the obstacle, and weeds grow thickly there. The gravel field has few weeds with low length. The experimental procedure is as follows. The ATV starts with the target constant speed of 5 [km/h]. When 10 seconds have past, the target steering angle is commanded to the steering control system. The whole data is recorded in the meantime.

Figure 23 shows the experimental results of the grass field. The actual steering angle is delayed from the target steering angle. It is considered that it would be affected by the self-aligning torque, the loss of the friction between the wire and the wire outer, and the loss of the friction between the tires and the ground surface. It seems that the output power of the steering device is insufficient since the wire tension is about to reach the maximum tension 150 [N].

Figure 24 shows the experimental results of gravel field. Compared with the experimental result of Grass field, it can be confirmed that the actual steering angle follows the target steering angle well. The steering torque tends to be lower than the grass field. It is considered that the land has less weed and friction between the tires and ground would be lower.

Fig.21 Grass field

Fig.22 Gravel field

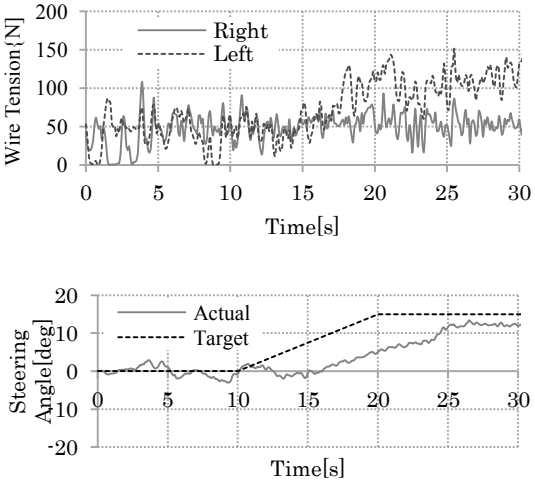

Fig.23 Steering angle control result at grass field

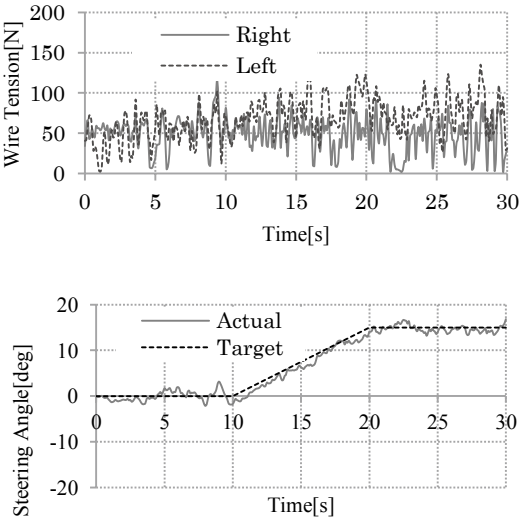

Fig.20 Steering angle control result at gravel ground field

6 CONDCLUDING REMARKS

In this study, as a part of the development of the autonomous mobile robot using an ATV to improve the efficiency of field survey activities, we constructed the steering angle control system and evaluated it. First of all, we introduced the CAN bus network for the distributed control system. Then we installed the steering angle control system and devices on the ATV after the evaluation on the test bed of the developed system. The steering angle control system realizes tracking the target values; however it is considered that the response speed greatly influenced by terrain.

In the next step, we have been evaluating and adjusting the steering control system. Development of the environmental measurement equipment is the future work.

7 ACKNOWLEDGE

This research was subsidized by the Center of Environmental Science and Disaster Migation for Advanced Research, Muroran Institute of Technology. The authors would like to thank here. Finally, the authors are deeply thankful to Suzuki Motor Corporation, who willingly lent the ATV indispensable to this research.

REFERENCE

(1) E. F. Fukushima, P. Debenest, S.Hirose, Development of Gryphon-I: Autonomous Buggy Robot for Off-Road Applications, Proc. Of 2002 JSME conf. on Robotics and Mechatronics, pp. 2A1-J09(1)-(2) (2002)

(2) T. Fujita, T. Takahashi, Development of Wall Surface Decontamination Robot in Nuclear Power Plant, Transactions of the Atomic Energy Society of Japan 3(2), 208-214, (2004)

(3) S. Kawano, K.Nakano, N. Kishikawa, T. Kudou, R. Tanoka, Development of UNDER-WATER ROBOT for Research of Lake, Proceedings of The 41st Conference of The Japan Society of Mechanical Engineers-Chugoku-Shikoku Branch, pp.405-406, (2003)

(4) Y. Wakabayashi,N. Yoshioka, Remote Driving Technology for a Lunar Rover : Lunar Rover Robotics Technology, Institute of Electronics, Information and Communication Engineers, Vol. 96, NO. 142, pp. 19-24 (1996)

(5) S.Hirose, F.Matsuno, Development of Snake Robots for Rescue Operation : Design of the Shape and Its Control, Journal of the Japan Society of Mechanical Engineers, Vol.106, No.1019, pp.769-773, (2003)

(6) T. Akiba,T. Michishita, Y. Tochikubo, N.Hanajima, H. Hikita, and M. Yamashita, Development and control of autonomous vehicles based on the ATV, Proc.of Hokkaido Branch Annual Conference 42th SICE, pp.57-60, A-23, (2010)

(7) T. Michishita, T. Akiba, Y. Tochikubo, N.Hanajima, H. Hikita, and M. Yamashita, Development of a wire winding steering system for an autonomous All Terrain Vehicle, Proc.of Hokkaido Branch Annual Conference 42th SICE, pp.61-62, A-24, (2010)

(8) T. Kamiya, H. Imai, Y. Masuda, Development of the "UGV" Unmanned Vehicle Incorporating Technologies of the Ubiquitous Computing Realm, Yamaha Mot Tech Rev, NO.39, pp.34-38, (2005)

(9) Y. Tsushiya, M. Mizukawa T. Suehiro, N.i Ando H. Nakamoto, A. Ikezoe, Construction of the CAN module composition type robot using RT-Middleware, 7th SICE System Integration Division Annual Conference, pp. 964-965, (2006)

(10) Y. Tochikubo, N.Hanajima, H. Hikita, and M. Yamashita, System integration in autonomous ATV by CAN communication, 11th SICE System Integration Division Annual Conf, pp.1P1-D17 A-2010, (2010)

(11) M.Kobayashi, Y.Tochikubo, Y.Taruumi, J.Dai, N.Hanajima, M.Yamashita, Development of a steering system on the ATV -Development of control device using PSoCs-, Research Comittee on Robot Technolody in Hokkaido 4th Annual Conference, pp.148-152, P3-3, (2010)